

PAPER • OPEN ACCESS

Flexural dynamic behavior of submerged cylindrical structures under wave loads

To cite this article: T Giotis *et al* 2019 *IOP Conf. Ser.: Mater. Sci. Eng.* **700** 012022

View the [article online](#) for updates and enhancements.

Flexural dynamic behavior of submerged cylindrical structures under wave loads

T Giotis ^{1,2,*}, D Pavlou ¹ and K A Belibassakis ²

¹Dept. of Mechanical and Structural Engineering and Materials Science, University of Stavanger, Norway

²School of Naval Architecture and Marine Engineering, National Technical University of Athens, Greece

* Corresponding author: fanisgiotis@gmail.com

Abstract. An analytical solution for the dynamic response of submerged slender circular cylindrical structure subjected to linear wave loads is presented. A double Laplace transform with respect to temporal and spatial variables is applied both to motion equation and boundary conditions. The dynamic deflection of the beam is obtained by inversion of the Laplace transform. The latter with respect to spatial variable is obtained analytically, while the one concerning the temporal variable is numerically calculated using Durbin numerical scheme. Results in the case of a representative example for a monopile foundation subjected to Airy waves are presented and discussed, and the analytical result is compared against numerical dynamic and static solutions.

1. Introduction

The analysis of dynamic response of circular cylindrical structures under wave loads has attracted attention by many investigators. The focus is mainly on the determination of dynamic deflection obtained through numerical methods, and experimental studies in wave tank, e.g., [1]. In the present work an analytical solution for the dynamic response of slender cylindrical structures under Airy waves is presented, which is obtained by using Laplace transform techniques. The proposed solution has the advantage that the solution of the PDE is analytic and could be easily extended to include the additional effect of current. Formulation of the problem is valid for rocky or stiff seabed. The waves encountered in the installation area are characterized by a small steepness ratio H/λ and as a result they can be considered as linear. The mono-pile foundation is assumed fixed on the seabed. This assumption The geometric characteristics of the pile remain constant throughout its length and the outer diameter (D_{out}) of the foundation is small with respect to the wavelength (λ) of the installation area. The small ratio H/λ allows the assumption that the flow disturbance is not significant due to the presence of the structure and as a result, the monopile can be considered as a slender structure. The origin (O) of the system is located on the center of the foundation base (Figure 1).



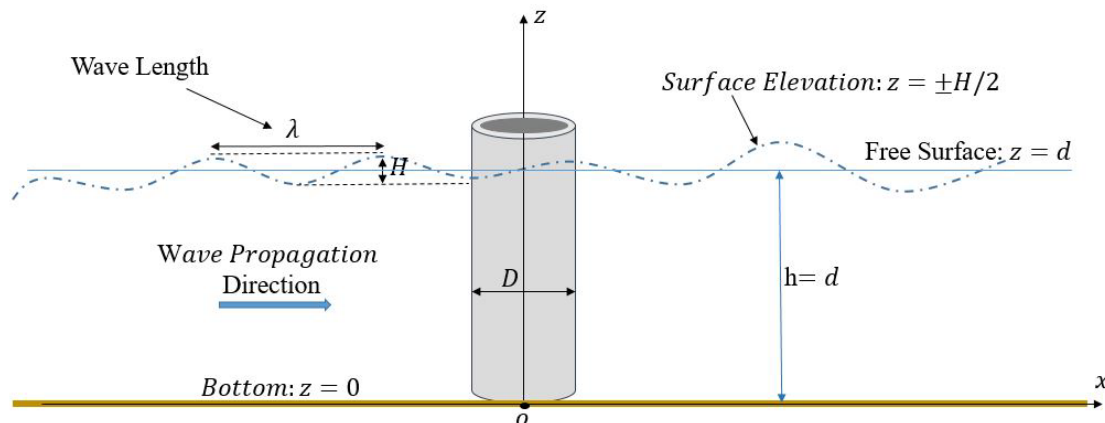


Figure 1. The origin system of the monopile.

2. Analytical solution of the problem

2.1 Boundary conditions

The fixed end which is located on the seabed $z = 0$. Thus, slope and deflection are zero at $z = 0$.

$$w(0, t) = \frac{\partial w(z, t)}{\partial z} \Big|_{z=0} = 0 \tag{1}$$

The upper end at $z = L$ is free and as a result, both bending moment and shear force are zero at $z = L$.

$$E \cdot I(z) \cdot \frac{\partial^2 w(z, t)}{\partial z^2} \Big|_{z=L} = 0 \tag{2}$$

$$\frac{\partial}{\partial z} \left[E \cdot I(z) \cdot \frac{\partial^2 w(z, t)}{\partial z^2} \right] \Big|_{z=L} = 0 \tag{3}$$

2.2 Equation of motion

The dynamic displacement field is expressed by means of Euler-Bernoulli beam model [2]:

$$E \cdot I \cdot \frac{\partial^4 w(z, t)}{\partial z^4} + P \cdot A \cdot \frac{\partial^2 w(z, t)}{\partial t^2} + C \cdot \frac{\partial w(z, t)}{\partial t} = q(z, t) \tag{4}$$

The right hand side part of (4) is the hydrodynamic load is calculated by using potential wave theory [3, 4] and Morison Equation [5]. The circular cylinder is considered as a moving structure in waves. Thus, the relative formulation of Morison Equation is used. However, the structure represents a monopile offshore wind turbine, which has to be rigid enough for the safety of the rotor. The rigidity of the structure ensures that the maximum deflection amplitude is much smaller than the structure diameter (D_{out}), and as a result, the velocity of the structure could be neglected. The final form of the hydrodynamic load is given by (5).

$$q(z, t) = -\rho \times C_A \times A \times \frac{\partial^2 w(z, t)}{\partial t^2} + \rho \times C_M \times A \times \frac{Du(t)}{Dt} + \frac{1}{2} \times \rho \times C_D \times D_{out} \times u(t) \times |u(t)| \tag{5}$$

The drag term of Eq. (5) is linearized and the final form of equation of motion is:

$$\begin{aligned}
& E \cdot I \cdot \frac{\partial^4 w(z, t)}{\partial z^4} + [P \cdot A + \rho \cdot C_A \cdot A] \cdot \frac{\partial^2 w(z, t)}{\partial t^2} + C \cdot \frac{\partial w(z, t)}{\partial t} = \\
& -C_M \cdot \rho \cdot \frac{\pi \cdot D_{out}^2}{4} \cdot \omega^2 \cdot \frac{H}{2} \cdot \frac{\cosh(k \cdot z)}{\sinh(k \cdot d)} \cdot \sin(\omega \cdot t) + \frac{1}{2} \cdot \rho \cdot C_D \cdot D \cdot \left[\frac{H}{2} \cdot \omega \cdot \frac{\cosh(k \cdot z)}{\sinh(k \cdot d)} \right]^2 \cdot \cos(\omega \cdot t) \quad (6)
\end{aligned}$$

2.3 General solution of the motion equation

For the solution of the boundary value problem, Laplace transform will be applied to the spatial and temporal variables. The definition of these transforms and their inverse forms used on the solution is given in the Appendix. Application of the Laplace transform with respect to time and introduction of $w^{(n)}(z, 0) = 0$ for $n=1, 2, 3, 4$ yield:

$$\begin{aligned}
& E \cdot I \cdot \frac{\partial^4 w^*(z, s)}{\partial z^4} + w^*(z, s) \cdot [(P \cdot A_C + \rho \cdot C_A \cdot A) \cdot s^2 + C \cdot s] = \\
& -C_M \cdot \rho \cdot \frac{\pi \cdot D_{out}^2}{4} \cdot \omega^3 \cdot \frac{H}{2} \cdot \frac{\cosh(k \cdot z)}{\sinh(k \cdot d)} \cdot \left(\frac{1}{s^2 + \omega^2} \right) + \frac{1}{2} \cdot \rho \cdot C_D \cdot D \cdot \left[\frac{H}{2} \cdot \omega \cdot \frac{\cosh(k \cdot z)}{\sinh(k \cdot d)} \right]^2 \cdot \left(\frac{s}{s^2 + \omega^2} \right) \quad (7)
\end{aligned}$$

where

$$w^*(z, s) = \mathcal{L} \{ w(z, t); t \rightarrow s \} = \int_0^{\infty} e^{-s \cdot t} \cdot w(z, t) dt \quad (8)$$

Application of the Laplace transform with respect to z and introduction of zero initial conditions into (7) yield:

$$\begin{aligned}
& E \cdot I \cdot \left[-\bar{w}'''(0, s) - q \cdot \bar{w}''(0, s) - q^2 \cdot \bar{w}'(0, s) - q^3 \cdot \bar{w}(0, s) + q^4 \cdot \bar{w}^*(q, s) \right] + \\
& [(P \cdot A + \rho \cdot C_A \cdot A) \cdot s^2 + C \cdot s] \cdot \bar{w}^*(q, s) = \\
& -C_M \cdot \rho \cdot \frac{\pi \cdot D_{out}^2}{4} \cdot \omega^3 \cdot \frac{H}{2} \cdot \frac{1}{\sinh(k \cdot d)} \cdot \left(\frac{1}{s^2 + \omega^2} \right) \cdot \left(\frac{q}{q^2 - k^2} \right) + \\
& \frac{1}{8} \cdot C_D \cdot \rho \cdot D_{out} \cdot H^2 \cdot \omega^2 \cdot \frac{1}{\sinh^2(k \cdot d)} \cdot \left(\frac{s}{s^2 + \omega^2} \right) \cdot \frac{q^2 - 2 \cdot k^2}{q \cdot (q^2 - 4 \cdot k^2)} \quad (9)
\end{aligned}$$

where

$$\bar{w}^*(q, s) = \mathcal{L} \{ w^*(z, s); z \rightarrow q \} = \int_0^{\infty} e^{-q \cdot z} \cdot w^*(z, s) \cdot dz \quad (10)$$

For the simplification of (9), the Laplace transform is applied into the boundary conditions (2). Thus, the conditions at $z=0$ takes the following form:

$$\bar{w}(0, s) = \mathcal{L} \{ w(0, t); t \rightarrow s \} = 0 \quad (11)$$

$$\bar{w}'(0, s) = \mathcal{L} \{ w'(0, t); t \rightarrow s \} = 0 \quad (12)$$

Introducing Eqs. (11), (12) into Eq. (9) yields:

$$\begin{aligned} \bar{w}^*(q,s) \cdot \left[E \cdot I \cdot q^4 + (P \cdot A + \rho \cdot C_A \cdot A) \cdot s^2 + C \cdot s \right] = E \cdot I \cdot q \cdot \bar{w}''(0,s) + E \cdot I \cdot \bar{w}'''(0,s) - \\ C_M \cdot \rho \cdot \frac{\pi \cdot D_{out}^2}{4} \cdot \omega^3 \cdot \frac{H}{2} \cdot \frac{1}{\sinh(k \cdot d)} \cdot \left(\frac{1}{s^2 + \omega^2} \right) \cdot \left(\frac{q}{q^2 - k^2} \right) + \\ \frac{1}{8} \cdot C_D \cdot \rho \cdot D_{out} \cdot H^2 \cdot \omega^2 \cdot \frac{1}{\sinh^2(k \cdot d)} \cdot \left(\frac{s}{s^2 + \omega^2} \right) \cdot \frac{q^2 - 2 \cdot k^2}{q \cdot (q^2 - 4 \cdot k^2)} \end{aligned} \quad (13)$$

Solving (13) with respect to $\bar{w}^*(q,s)$, yields:

$$\bar{w}^*(q,s) = \bar{M}_1^*(q,s) \cdot \bar{w}''(0,s) + \bar{M}_2^*(q,s) \cdot \bar{w}'''(0,s) + \bar{M}_3^*(q,s) + \bar{M}_4^*(q,s) \quad (14)$$

where

$$\bar{M}_1^*(q,s) = \frac{q}{q^4 + \frac{(P \cdot A + \rho \cdot C_A \cdot A) \cdot s^2 + C \cdot s}{E \cdot I}} \quad (15)$$

$$\bar{M}_2^*(q,s) = \frac{1}{q^4 + \frac{(P \cdot A + \rho \cdot C_A \cdot A) \cdot s^2 + C \cdot s}{E \cdot I}} \quad (16)$$

$$\bar{M}_3^*(q,s) = - \frac{C_M \cdot \rho \cdot \frac{\pi \cdot D_{out}^2}{4} \cdot \omega^3 \cdot \frac{H}{2} \cdot \frac{1}{\sinh(k \cdot d)} \cdot \left(\frac{1}{s^2 + \omega^2} \right) \cdot \left(\frac{q}{q^2 - k^2} \right)}{E \cdot I \cdot q^2 + (P \cdot A + \rho \cdot C_A \cdot A) \cdot s^2 + C \cdot s} \quad (17)$$

$$\bar{M}_4^*(q,s) = \frac{\frac{1}{8} \cdot C_D \cdot \rho \cdot D_{out} \cdot H^2 \cdot \omega^2 \cdot \frac{1}{\sinh^2(k \cdot d)} \cdot \left(\frac{s}{s^2 + \omega^2} \right) \cdot \left(\frac{q^2 - 2 \cdot k^2}{q \cdot (q^2 - 4 \cdot k^2)} \right)}{E \cdot I \cdot q^4 + (P \cdot A + \rho \cdot C_A \cdot A) \cdot s^2 + C \cdot s} \quad (18)$$

Application of the inverse Laplace transform with respect to q into Eq. (14) yields:

$$\bar{w}(z,s) = \bar{M}_1(z,s) \cdot \bar{w}''(0,s) + \bar{M}_2(z,s) \cdot \bar{w}'''(0,s) + \bar{M}_3(z,s) + \bar{M}_4(z,s) \quad (19)$$

where

$$\bar{w}(q,s) = \mathcal{L}^{-1} \left\{ \bar{w}^*(q,s); q \rightarrow z \right\} \quad (20)$$

$$\bar{M}_i(z,s) = \mathcal{L}^{-1} \left\{ \bar{M}_i^*(q,s); q \rightarrow z \right\}, \quad i = 1, 2, 3, 4 \quad (21)$$

Equation (19) contains two unknown variables $\bar{w}''(0,s)$ and $\bar{w}'''(0,s)$. The first expresses the bending moment at the position $z=0$ and the second is equal with the shear force at the base of the foundation ($z=0$). The determination of those variables is achieved by the introduction of the boundary conditions of the beam at the position $z=L$. Application of the Laplace transform with respect to time into Eqs. (2) and (3) yields:

$$\bar{w}''(L,s) = L \{ w''(L,t); t \rightarrow s \} = 0 \quad (22)$$

$$\bar{w}'''(L,s) = L \{ w'''(L,t); t \rightarrow s \} = 0 \quad (23)$$

Introduction of Eq. (25) and (26) into Eq. (19) yields:

$$\bar{w}''(0,s) = \frac{\left[\bar{M}_3'''(L,s) + \bar{M}_4'''(L,s) \right] \cdot \bar{M}_2''(L,s) - \left[\bar{M}_3''(L,s) + \bar{M}_4''(L,s) \right] \cdot \bar{M}_2'''(L,s)}{\bar{M}_2'''(L,s) \cdot \bar{M}_1''(L,s) \cdot \left[1 - \frac{\bar{M}_2''(L,s) \cdot \bar{M}_1'''(L,s)}{\bar{M}_2'''(L,s) \cdot \bar{M}_1''(L,s)} \right]} \quad (24)$$

$$\bar{w}'''(0,s) = - \frac{\left[\bar{M}_3'''(L,s) + \bar{M}_4'''(L,s) \right] \cdot \bar{M}_2''(L,s) - \left[\bar{M}_3''(L,s) + \bar{M}_4''(L,s) \right] \cdot \bar{M}_2'''(L,s)}{\bar{M}_2'''(L,s) \cdot \bar{M}_1''(L,s) \cdot \left[1 - \frac{\bar{M}_2''(L,s) \cdot \bar{M}_1'''(L,s)}{\bar{M}_2'''(L,s) \cdot \bar{M}_1''(L,s)} \right]} \times$$

$$\frac{\bar{M}_1'''(L,s)}{\bar{M}_2'''(L,s)} - \frac{\bar{M}_3'''(L,s) + \bar{M}_4'''(L,s)}{\bar{M}_2'''(L,s)} \quad (25)$$

Application of the inverse Laplace transform with respect to s into (19) finally yields:

$$w(z,t) = L^{-1} \left\{ \bar{M}_1(z,s) \cdot \bar{w}''(0,s) + \bar{M}_2(z,s) \cdot \bar{w}'''(0,s) + \bar{M}_3(z,s) + \bar{M}_4(z,s); s \rightarrow t \right\} \quad (26)$$

where

$$w(z,t) = L^{-1} \left\{ \bar{w}(z,s); s \rightarrow t \right\} \quad (27)$$

2.4 Linearization of the hydrodynamic load

It is important to mention that the equation which describes the horizontal Drag load on strip is a non-linear equation. The analytical calculation of the pylon response under the horizontal wave loads requires the formulation of the load equation as the addition of linear harmonic terms. It can be achieved by developing the Drag load into a Fourier series. The process of converting the Drag load into a sum of linear harmonic terms is described in detail as follows. Non-linear term could be written as an independent function named N .

$$N = C_2 \left| \cos(k x_c - \omega t) \right| \cos(k x_c - \omega t) \quad (28)$$

where

$$C_2 = \frac{1}{2} \cdot \rho \cdot C_D \cdot D_{out} \cdot \left[\frac{H}{2} \cdot \omega \cdot \frac{\cosh[k \cdot (z + d)]}{\sinh(k \cdot d)} \right]^2$$

By setting $\theta = k \cdot x_c - \omega \cdot t$, (28) takes the following form:

$$N(\theta) = C_2 \cdot |\cos(\theta)| \cdot \cos(\theta) \Rightarrow N(\theta) = \begin{cases} C_2 \cdot \cos^2(\theta), & -\frac{\pi}{2} \leq \theta \leq \frac{\pi}{2} \\ -C_2 \cdot \cos^2(\theta), & \frac{\pi}{2} \leq \theta \leq \frac{3 \cdot \pi}{2} \end{cases} \quad (29)$$

Let us now consider the representation of $N(\theta)$ in a Fourier series as follows:

$$\frac{N(\theta)}{C_2} = \frac{1}{2} \cdot a_0 + \sum_{j=1}^{\infty} a_j \cdot \cos(j \cdot \theta) + \sum_{j=1}^{\infty} b_j \cdot \sin(j \cdot \theta) \quad , \quad \text{where } a_j = \frac{2}{\pi} \cdot \int_0^{\pi} N(\theta) \cdot \cos(j \cdot \theta) \cdot d\theta ,$$

$$\text{and } b_j = \frac{2}{\pi} \cdot \int_0^{\pi} N(\theta) \cdot \sin(j \cdot \theta) \cdot d\theta .$$

In the case when $a_0=0$ and $|a_j| \ll |a_1|$, and $|b_j| \ll |b_1|$, for $j > 1$, as happens to be the ones considered here, the function $N(\theta)$ is approximated by using only the first term in the series as follows:

$$\frac{N(\theta)}{C_2} \gg a_1 \cdot \cos(\theta), \quad \text{with } a_1 = \max \left| \frac{N(\theta)}{C_2} \right| \quad (30)$$

Using the above approximation in Eq. (5) we finally obtain:

$$\frac{dF_{N_D}(t)}{dz} \approx \frac{1}{2} \cdot \rho \cdot C_D \cdot D_{out} \cdot \left[\frac{H}{2} \cdot \omega \cdot \frac{\cosh[k \cdot (z + d)]}{\sinh(k \cdot d)} \right]^2 \cdot \cos(k \cdot x_c - \omega \cdot t) \quad (31)$$

3. Numerical example of the analytical solution

A vertical circular cylindrical structure, fixed in the seabed is considered, as described by Table 1.

Table 1. Structural characteristics of the pile.

Magnitude	Name	Value
Height (m)	h	30
Outer Diameter (m)	D_{out}	6
Shell Thickness (m)	thik	0.05
Modulus of Elasticity (GPa)	E	210
Poisson's Ratio	v	0.30
Density of Material (kg/m^3)	P	7820
Damping Coefficient	C	4398
Added Mass Coefficient	C_A	1
Drag Coefficient	C_D	0.65

The wave characteristics of the installation area of the structure are given in Table 2.

Table 2. Wave characteristics of the installation area.

Magnitude	Name	Value
Wave Height (m)	H	3.5
Wave Period (sec)	T	6
Water Depth (m)	d	30
Wavenumber	k	0.1121
Wave Frequency (rad/sec)	w	1.0472
Density of Water (kg/m ³)	ρ	1024.7

The comparison of the non-linear drag load at the top of the structure ($z = h$) and its linearized approximation by means of (31) is presented in Figure 2.

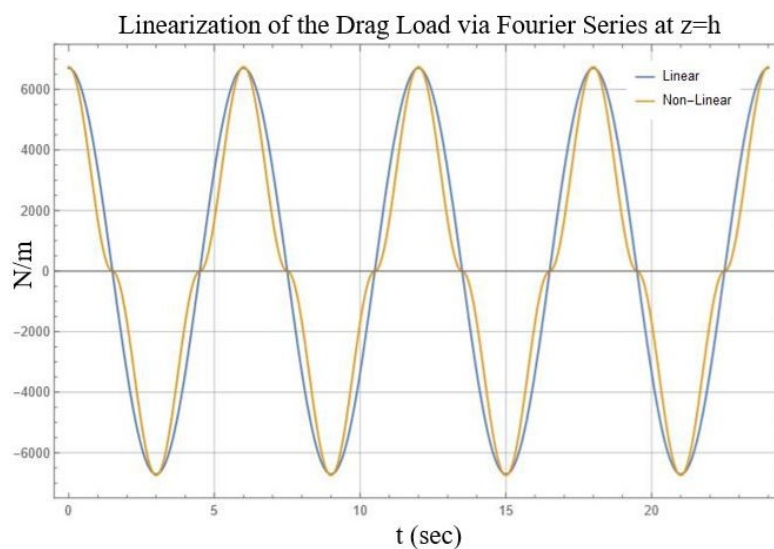


Figure 2. Linear and non-linear drag load at $z = h$.

Applying the Morison Equation for both linear and non-linear drag load, the total hydrodynamic load on the top of the structure ($z = h$) is presented in Figure 3.

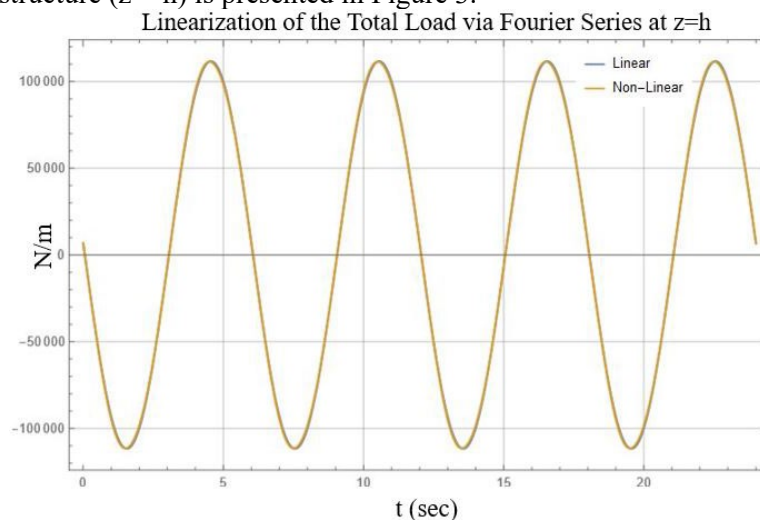


Figure 3. Linear and non-linear total load at $z = h$.

Applying (23), the deflection of the structure at $z = h$, during four periods, is given in Figure 4.

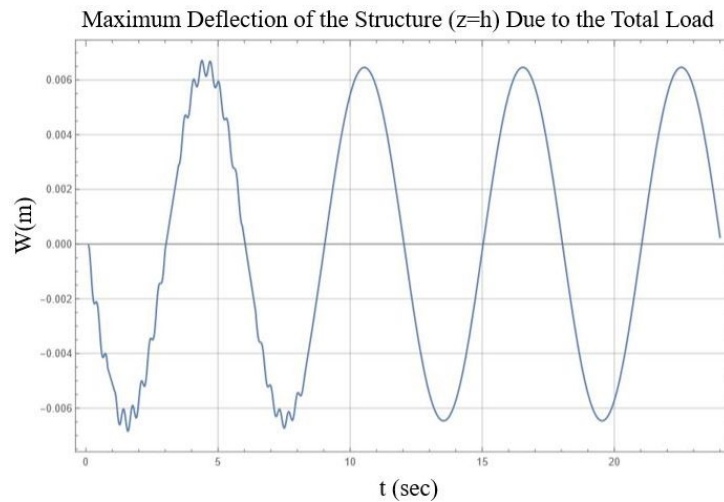


Figure 4. Deflection of the structure at $z = h$.

The response of the structure at $z = h$ follows the form of the total hydrodynamic load. Deflection is equal with zero at $t = 0$ due to the zero initial conditions used during the analytical solution. Thus, the maximum dynamic deflection of the beam is equal to $w(L)_{\text{Dynamic}} = 0.0064$ m. The calculated deflection of the pillar due to the hydrodynamic load is presented in Figure 5 for one period (T).

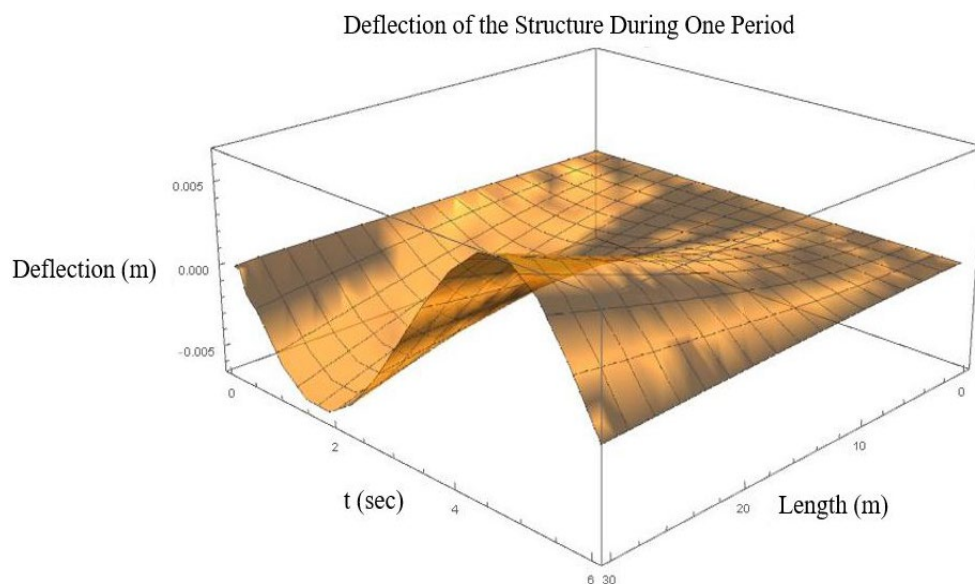


Figure 5. Deflection of the structure during one period.

4. Evaluation of the analytical solution

4.1 Comparison between analytical dynamic and static solution

To verify the reliability of the results, the dynamic maximum deflection of the structure due to the hydrodynamic load, is compared with the maximum static deflection. The solution of the static problem is achieved by using the finite element method (FEM). The maximum static deflection is $w(L)_{\text{Static}} = 0.0064$ m, and compared with the static maximum deflection, they are the equal. The dynamic deflection

of the beam with respect to the maximum static deflection due to the hydrodynamic load, is presented in Figure 6.

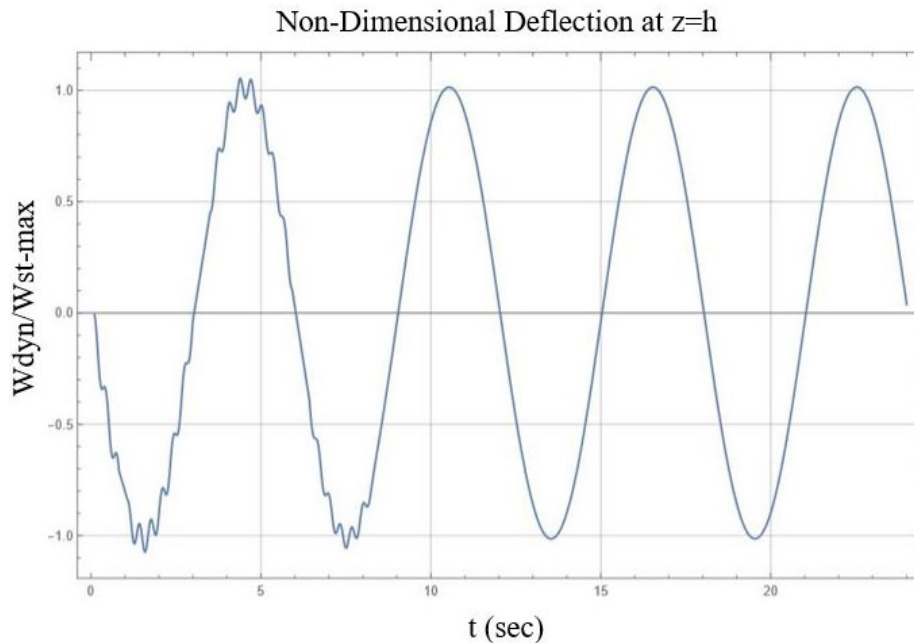


Figure 6. Comparison between maximum static and the dynamic deflection.

4.2 Comparison between analytical and numerical solution

For the validation of the present analytical model, the problem is also solved numerically by a Finite Differential Method, and the comparison between the numerical and analytical solution is presented in Figure 7. The numerical solution with FDM, verifies that the analytical solution is characterized by high accuracy.

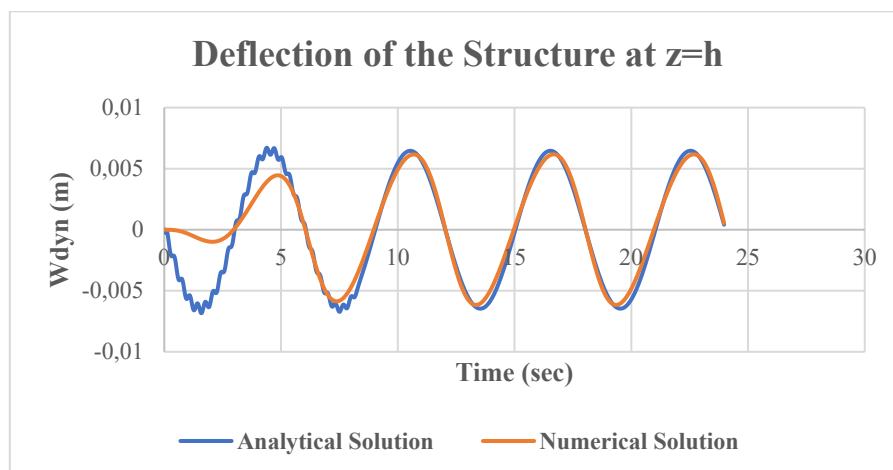


Figure 7. Comparison between numerical and analytical solution.

5. Conclusions

In this work the calculation of wave loads on slender vertical cylindrical structures is presented, as obtained by application of Morison Equation, in conjunction with potential flow theory. Results of representative examples for a monopile foundation subjected to short waves are presented and discussed. Subsequently, the elastic response of the vertical pillar in waves is studied and an analytical solution concerning the dynamic response is also derived based on linearization. For the validation of the present method, a numerical solution for the dynamic response of the monopile foundation subjected to general wave loads is derived, based on finite difference method (FDM). The numerical and the analytical solution give approximately the same result, verifying the accuracy of the analytical solution for waves of relatively small amplitude. Moreover, the calculation of the maximum static deflection of the structure subjected to the maximum wave loads is obtained by the finite element method (FEM) and is found compatible with the amplitude of analytical dynamic deflection.

Future work includes the introduction of current effects and wind loads into the analytical and numerical model which is important for a more efficient and realistic estimation of the dynamic response of such structures. Also, the developed analytical solution is realistic in the case of a seabed characterized by high stiffness due to the choice of fixed boundary condition at the base of the structure. For more realistic modelling of seabed material and foundation, enhanced boundary condition can be used.

References

- [1]. El Kaddah N H 1983 *Water wave-structure interaction for small amplitude structural oscillations*. Doctoral thesis, City University London.
- [2]. Graff K F 1975 *Wave motions in elastic solids*, Clarendon Press.
- [3]. Massel S.R, (1989). *Hydrodynamics of Coastal Zones*, Elsevier.
- [4]. Dean R G, Dalrymple R A 1991 *Water wave mechanics for engineers and scientists*, World Scientific.
- [5]. Det Norske Veritas Recommended Practice DNV-RP-C205 (2010), *Environmental Conditions and Environmental Loads*, DNV-RP-C205, October 2010.
- [6]. Pavlou D G 2015 *Essentials of the Finite Element Method for Mechanical and Structural Engineers*, Elsevier.
- [7]. Oberhettinger F and Badii L 1973 *Tables of Laplace Transforms*. Berlin Heidelberg, New York.
- [8]. Cheng H-D, Sidauruk P 1994 Approximate Inversion of the Laplace Transform, *The MATHEMATICA J.*, **4**(2) 76 - 82.

Appendix

The Laplace transform (with respect to z) of a function $f(z)$ is defined as

$$\mathcal{L}\{f(z); z \rightarrow p\} = \bar{f}(p) = \int_0^{\infty} f(z) \cdot e^{-p \cdot t} \cdot dp \quad (\text{A.1})$$

and its inverse is

$$f(z) = \mathcal{L}^{-1}\left\{\bar{f}(p); p \rightarrow z\right\} = \frac{1}{2 \cdot \pi \cdot i} \int_{\gamma-i\infty}^{\gamma+i\infty} \bar{f}(p) \cdot e^{p \cdot t} \cdot dp \quad (\text{A.2})$$

The Durbin method [8] for numerical inversion of Laplace transform approximates the time function $f(t)$ by a periodic function of period T . In the present case the following representation is used

$$f(t) \approx \frac{e^{at}}{T} \cdot \left\{ \frac{F(a)}{2} + \sum_{k=1}^N \operatorname{Re} \left[F \left(a + \frac{i\pi k}{T} \right) \cos \left(\frac{i\pi k}{T} \right) \right] - \operatorname{Im} \left[F \left(a + \frac{i\pi k}{T} \right) \sin \left(\frac{i\pi k}{T} \right) \right] \right\}, \quad (\text{A.3})$$

where $a = a - \frac{\ln E}{2T}$, E is the error tolerance, for which the default value $E = 1 \times 10^{-8}$ has been assigned,

and a is the real part of the leading pole of the function $F(s)$. For functions without poles, the default value $a = 0$ has been set.

The variables used in the paper are described in Table A1.

Table A1. Table of variables.

Magnitude	Symbol	Units
Outer Diameter	D_{out}	m
Shell Thickness	thick	m
Modulus of Elasticity	E	GPa
Poisson Ratio	ν	-
Density of Material	P	kg/m ³
Damping Coefficient	C	-
Deflection of the Structure	w	m
Added Mass Coefficient	C_A	-
Drag Coefficient	C_D	-
Wave Length	λ	m
Wave Frequency	ω	rad/sec
Wave Amplitude	H	m
Wave Period	T	sec
Water Depth	d	m
Density of Water	ρ	kg/m ³
Wavenumber	k	-